Indirect selective laser sintering of apatite–wollostonite glass–ceramic

K Xiao[1], **K W Dalgarno**[2*], **D J Wood**[3], **R D Goodridge**[4], and **C Ohtsuki**[5]
[1]School of Mechanical Engineering, University of Leeds, Leeds, UK
[2]School of Mechanical and Systems Engineering, Newcastle University, Newcastle upon Tyne, UK
[3]Dental Institute, University of Leeds, Leeds, UK
[4]Wolfson School of Mechanical and Manufacturing Engineering, Loughborough University, Loughborough, UK
[5]Department of Crystalline Materials Science, Graduate School of Engineering, Nagoya University, Nagoya, Japan

The manuscript was received on 19 February 2008 and was accepted after revision for publication on 2 April 2008.

DOI: 10.1243/09544119JEIM411

Abstract: This paper develops an indirect selective laser sintering (SLS) processing route for apatite–wollastonite (A–W) glass–ceramic, and shows that the processing route, which can create porous three-dimensional products suitable for bone implants or scaffolds, does not affect the excellent mechanical and biological properties of the glass–ceramic. 'Green parts' with fine integrity and well-defined shape have been produced from glass particles of single-size range or mixed-size ranges with acrylic binder in various ratios by weight. A subsequent heat treatment process has been developed to optimize the crystallization process, and an infiltration process has been explored to enhance mechanical strength. Three-point bending test results show flexural strengths of up to 102 MPa, dependent on porosity, and simulated body fluid (SBF) tests show that the laser sintered porous A–W has comparable biological properties to that of conventionally produced A–W.

Keywords: glass–ceramic, selective laser sintering, rapid manufacturing, bone repair, bioactivity

1 INTRODUCTION

As bones are not capable of fulfilling their repairing function automatically in many cases of major bone loss such as trauma, cancer, congenital abnormalities, or bone deficiency, the requirement for bone replacements to reconstruct bone tissues in the field of clinical application is attractive, because of the enhanced ability to salvage a massive loss of bone. Bioactive glass–ceramics, such as hydroxyapatite, have been widely used in bone substitution/regeneration fields [**1**] owing to their excellent bioactivity as well as superior mechanical properties. Conventionally sintered apatite–wollastonite (A–W) exhibits good mechanical properties, such as bending strength, which is around 200 MPa, almost twice that of sintered hydroxyapatite (HA) and even higher than the 160 MPa of human cortical bone [**2**]. Although conventional sintering can produce porous bone implants, the restriction and difficulties in the production of freeform shapes and customizable implants led to the adoption of an alternative fabrication technology in this study.

Selective laser sintering (SLS) has developed over the past two decades as a valuable technology in solid freeform fabrication (SFF). This technique is suitable for creating freeform three-dimensional (3D) porous structures, which can be tailored to be biomimetic in shape. In SLS, a 3D computer aided design (CAD) model is first sliced into a series of thin layers automatically. The data of these thin layers are then transferred from the computer to the SLS machine where these virtual layers are converted into physical layers through material deposition and bonding mechanisms. Two-dimensional (2D) layers are created by scanning a laser beam over a powder bed. The powder is heated and consolidated when

Corresponding author: School of Mechanical and Systems Engineering, Newcastle University, M18A Stephenson Building, Claremont Road, Newcastle upon Tyne, NE1 7RU, UK. email: kenny.dalgarno@ncl.ac.uk

the laser hits the powder bed. Further powder is then spread over the previously consolidated layer and the process repeated to make a second layer which, in addition to being consolidated, is bonded to the layer below. By repeating this process, 3D products are constructed.

There are two types of SLS production: direct SLS and indirect SLS. In direct SLS, powders are solely melted and consolidated by the laser. In indirect SLS, only a binder material is melted by the laser to bond powders, creating what is known in powder metallurgy terms as a 'green part'. Then, further heat treatment is used to sinter the powders and consolidate the structure. Indirect SLS of one type of glass–ceramic, apatite–mullite, has succeeded because of the good consolidation and porous structure achieved in this process [**3**]. This paper is concerned with applying the indirect SLS method to a new bioactive glass–ceramic, A–W, aiming to develop a material for hard tissue engineering, which has excellent mechanical properties and excellent bioactivity.

An advantage of the indirect SLS approach is that infiltration can be used to create composite materials, and in this study an examination has also been made of the creation of a ceramic–ceramic composite material, through using indirect SLS to create a porous A–W structure, and then infiltrating this structure with phosphate glass. Phosphate glass was chosen for two reasons. First, it has a lower melting point than A–W and so can be used as an infiltrant without affecting the A–W structure. Second, it is a rapidly resorbing material [**4**], as opposed to A–W which resorbs slowly [**5**], potentially creating a functional composite, with a rapidly resorbing phase to encourage bone ingrowth, with a long-term (but ultimately resorbable) structure to provide stability for an implant.

2 MATERIAL PREPARATION

The reagents used for producing A–W parent glass are MgO, SiO_2, P_2O_5, $CaCO_3$, and CaF_2. The ratio of each component in the most popular composition, reported by Kokubo *et al.* [**2**], is shown in Table 1. Note that $CaCO_3$ comes from the reaction of CaO with CO_2.

Table 1 Composition of A–W forming glass

	MgO	CaO	SiO_2	P_2O_5	CaF_2
Wt%	4.6	44.7	34.0	16.2	0.5
Mol%	7.1	49.9	35.5	7.1	0.4

The reagent powders, weighed on digital balance (Sartorius roughing balance), were mixed in a clean plastic container and then were rotated on a rolling machine for 1 h with an agitating iron bar inside. Then the mixture was dropped into an alumina crucible, which was then placed into a larger mullite crucible with lid. The reagents were melted in a furnace at 1450 °C for 2 h, before being quenched in cold water. Glass frits were collected by pumping through a sieve and dried overnight. Batches of glass frits achieved were then ground on a Gy–Ro Rotary Mill for a few minutes and sieved on a sieve stack and shaker (Octagon Digital) into different size ranges of glass particles. Two different powder mixtures were used in processing. The first (designated PM1) comprised A–W powder in the size range of 45–90 μm with 5 per cent by mass of an acrylic binder. The second powder mixture (designated PM2) used was 64 per cent of the 45–90 μm size range, with 21 per cent 0–45 μm size range and 15 per cent acrylic binder (percentages by mass).

The phosphate glass used in this research for the infiltration was produced from the molar composition of 50 per cent P_2O_5, 40 per cent CaO, 10 per cent Na_2O. Chemical reagents used for this production were P_2O_5, $CaCO_3$ and Na_2CO_3, the weight ratio of which is shown in Table 2.

The melting temperature for making phosphate glass is 1100 °C and the melting time was 1 h. The phosphate glass melts were poured within a steel ring on a smooth steel plate at room temperature and then covered by a steel lid. After cooling down, the glass lumps were ground and sieved into sub 45 μm particle sizes and stored in a desiccator before use.

3 PROCESSING

3.1 SLS processing

Indirect SLS processing was carried out on an experimental SLS machine, shown schematically in Fig. 1. This machine uses a 250 W CO_2 laser with a spot size at the powder bed of 0.6 mm or 1.1 mm. The establishment of a processing window in indirect SLS begins with establishing the processing parameters that cause ignition of the binder, and this was determined using a raster scan pattern with an

Table 2 Composition of phosphate glass

Reagents	P_2O_5	$CaCO_3$	Na_2CO_3
Mol%	50	40	10
Weight%	58.36	32.92	8.72

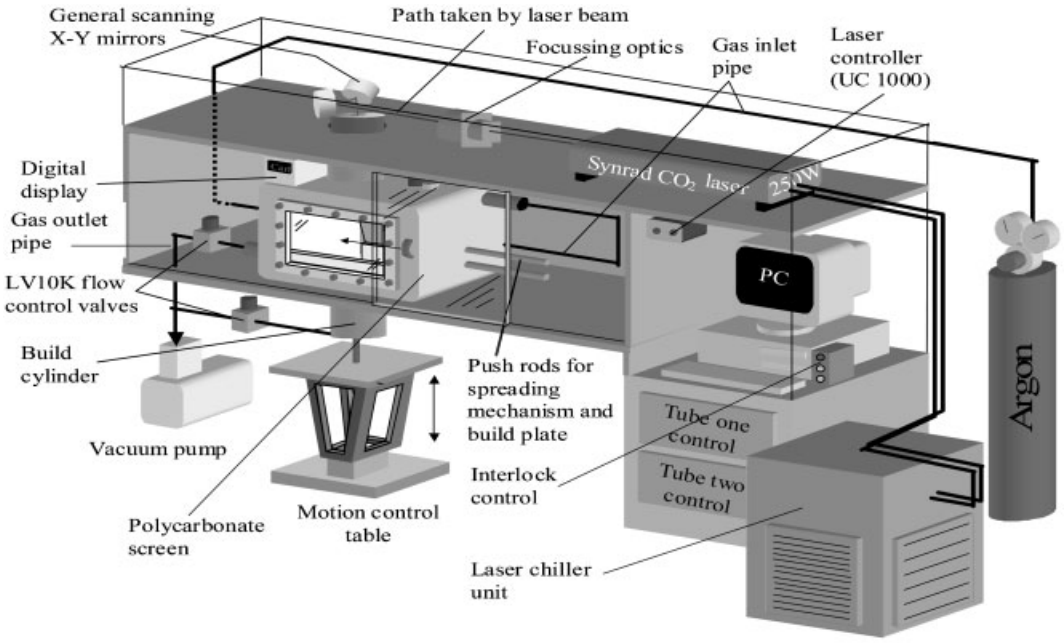

Fig. 1 Schematic of experimental SLS machine

overlap between adjacent scan lines of 50 per cent of the spot size at the powder bed. The thickness of powder layers spread in making scaffolds was 0.125 mm.

Figure 2 shows the process map which resulted for the production of single-layer components using PM1. Clearly the viable processing window lies below the ignition line for each laser beam diameter. On the basis of qualitative assessments of handling ability and strength of the 'green parts', processing conditions of 5 W and 150 mm/s were selected for the larger laser beam size, with the same power but a higher scan speed of 500 mm/s selected for the smaller laser beam size.

A similar process for PM2 resulted in processing conditions of 6 W and 150 mm/s being selected for processing of that powder mixture, which was only processed using the larger laser beam diameter.

Figures 3 and 4 illustrate the appearance and microstructure (observed by scanning electron microscopy, SEM) of a typical 'green part', processed using PM1 and a 1.1 mm laser beam diameter. Figure 4 clearly illustrates the irregular powder shape, which results from the powder production method.

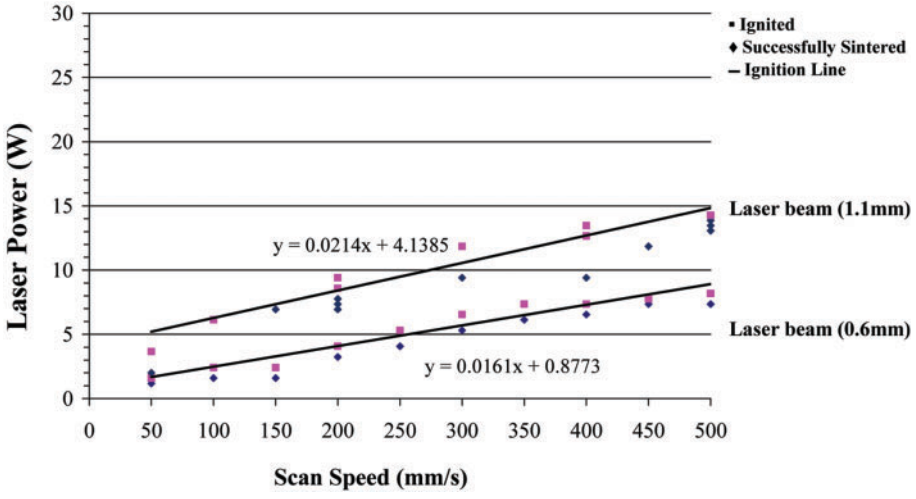

Fig. 2 Processing map for two different laser beam diameters. Scan spacing 50 per cent of beam diameter

Fig. 3 A 30-layer 'green part'. 15 mm × 15 mm × 3.8 mm

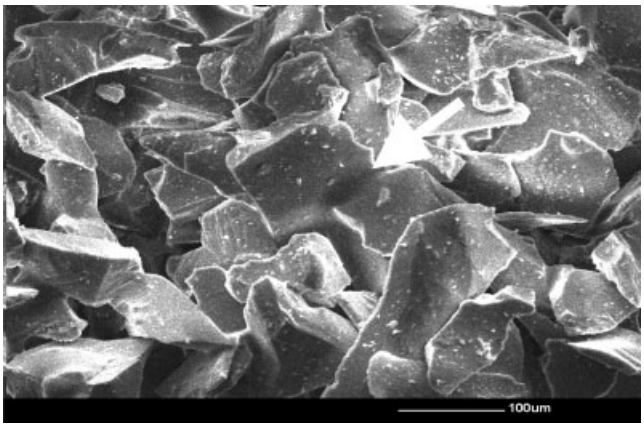

Fig. 4 SEM for multilayer 'green part'. Arrow indicates binder

3.2 Furnace processing

In post-processing, porous 'green parts' produced in SLS were taken through an optimized heat treatment process. The optimum nucleation temperature (ONT) and crystal propagation temperature were determined through differential thermal analysis (DTA) of the A–W glass with a heating rate of 10 K/min, as shown in Fig. 5.

The glass transition temperature was determined by the tangent method as 741 °C (similar to that reported by Likitvanichkul and Lacourse [**6**]). There are two obvious exothermic events at temperatures above 800 °C, which indicates that crystallization occurs with two crystal phases (apatite and wollastonite) generated. The crystallization phases were confirmed by X-ray diffraction (XRD).

In the heat treatment development, the ONT was determined as 779 °C for both the apatite and wollastonite phases with an optimum nucleation time of 1 h. The crystallization temperature was found to be 1150 °C. Therefore, a suitable heat treatment scheme developed for post-processing of the 'green parts' involves a hold of 1 h at 779 °C to optimize the nucleation process with a further hold of 1 h at 1150 °C to improve the propagation of crystal growth, especially for the precipitation of wollastonite. The heat treatment scheme is shown in Fig. 6 and Fig. 7 illustrates the microstructure that resulted from processing the 'green parts' this way (to produce 'brown parts'). Figure 7 can be contrasted with Fig. 4 to illustrate the effect of the heat treatment.

Figure 7 illustrates that the A–W structure is very porous, with typical levels of porosity of 40 per cent, assessed by weighing the parts and comparing the mass with that expected of fully dense parts with a similar volume. In order to produce scaffolds with a high mechanical strength, further infiltration with calcium phosphate glass was used as a secondary heat treatment for some samples. The calcium phosphate was placed on top of 'brown parts' and

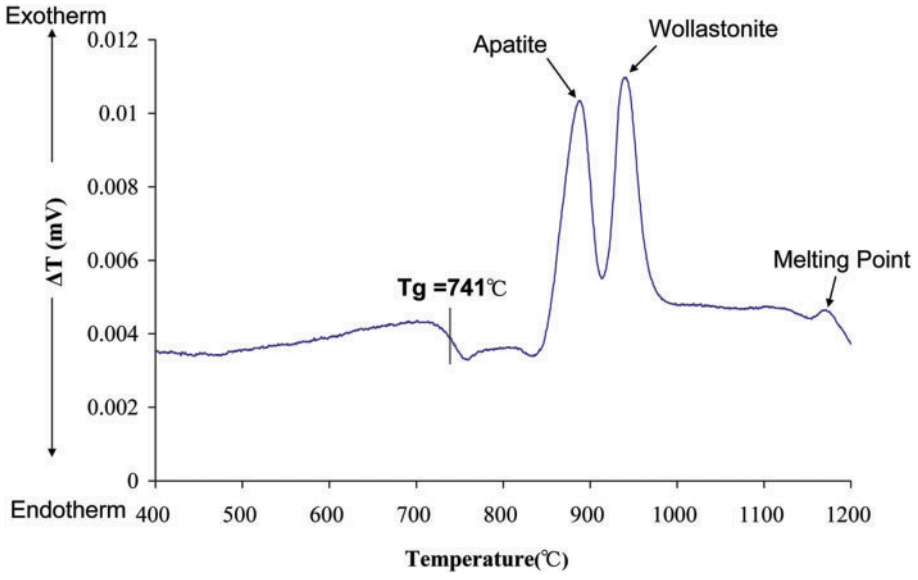

Fig. 5 DTA trace of A–W glass. Particle size range 45–90 μm. Heating rate 10 K/min

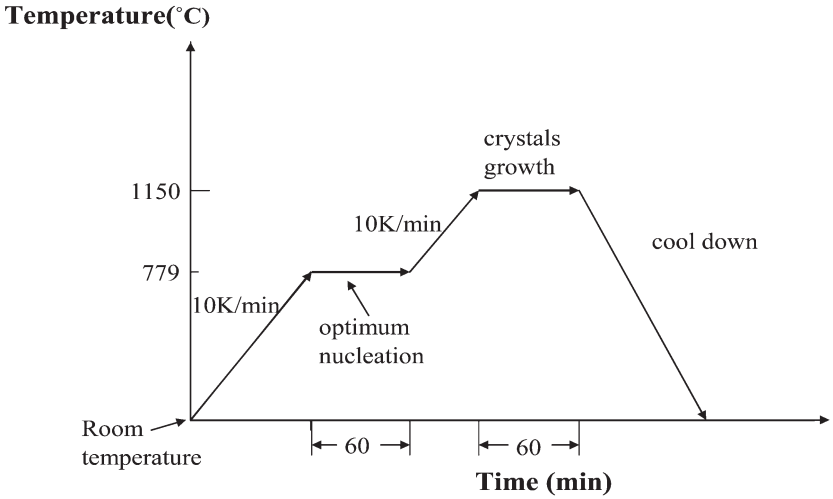

Fig. 6 Heat treatment scheme

the temperature raised to 900 °C in a vacuum furnace. This temperature is sufficient to melt the calcium phosphate glass, which then infiltrates into the 'brown part' under the action of gravity and capilliary forces [**7**]. Figure 8 shows the result of this process when applied to a brown part made from processing the PM2 material. The phosphate glass in this image is the darker of the two materials, with the lighter material being A–W.

4 CHARACTERIZATION

4.1 Mechanical characterization

The mechanical behaviour of the scaffolds has been assessed through three-point bend tests, performed as shown in Fig. 9. A calibrated 500 N ($\pm$5 per cent) load cell was used and jigs with roller supports with a 20 mm span were fitted. For three-point bending tests of A–W, beam-shape samples with nominal dimensions of 25 mm $\times$ 4 mm $\times$ 3 mm were fabricated. During the SLS stage samples were orientated such that the vertical height was the 3 mm dimension. All the tests were carried out under room conditions and the speed of the cross-head was 2 mm/min.

In the analysis of the three-point bend test results, fracture was identified by a sharp decrease of loading force in load–displacement plots and the peak force was used as the force for the calculation of flexural strength (σ_{fs}) via the equation shown below

$$\sigma_{fs} = \frac{3}{2}\frac{Pl}{ab^2}$$

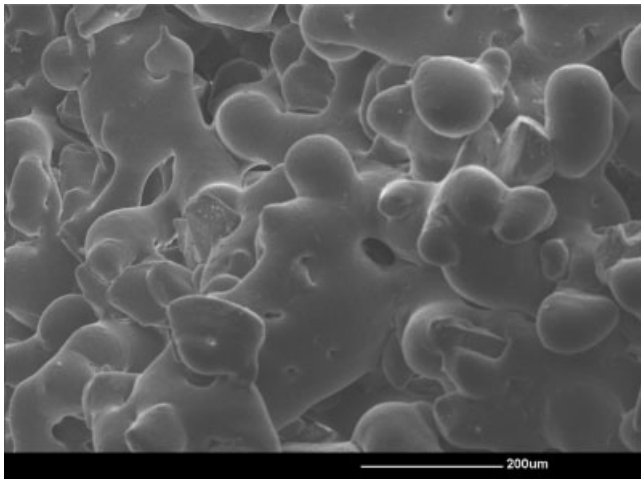

Fig. 7 SEM for multilayer 'brown part'

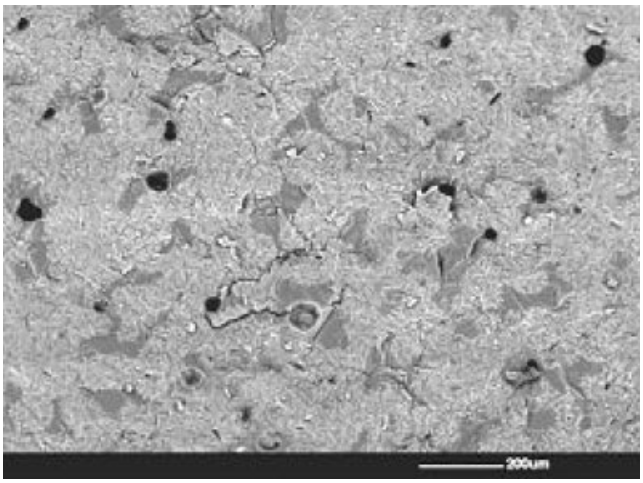

Fig. 8 SEM of infiltrated PM2 part

Fig. 9 Three-point bend test

where P is the loading force, l is the span of two parallel roller supports, a is the width of sample, and b is the thickness of sample.

Figure 10 shows the results of bend tests with PM1, PM2, and PM2 which has subsequently been infiltrated with the phosphate glass. The results show that these three materials cover most of the range of strengths which would be expected from natural bone, meaning that – through a combination of choice of powder mixture and postprocessing approach – scaffolds, which have properties tailored to a particular implantation site, could be produced.

4.2 Biocompatability

Before the use of a material in tissue engineering trials, basic biocompatibility must be investigated, and this has been carried out through simulated body fluid (SBF) testing, an established procedure for the assessment of biocompatibility [**8**].

Normal SBF with a pH of 7.25 at 36.5 °C was used. The samples prepared were blocks with dimensions of $15 \times 15 \times 2$ mm using PM1. The apparent surface area of all the samples was measured and the volume of SBF used for soaking was calculated according to the ratio of 0.1 ml SBF to 1 mm^2. Three samples of each material were used, each left for 1, 3, 7, or 14 days. The surface of the samples was characterized by SEM before and after soaking in SBF for each time period. The chemical composition and structure of any material deposited on the surface was studied by electron dispersive X-ray microanalysis (EDX) and thin-film X-ray diffraction (TF-XRD).

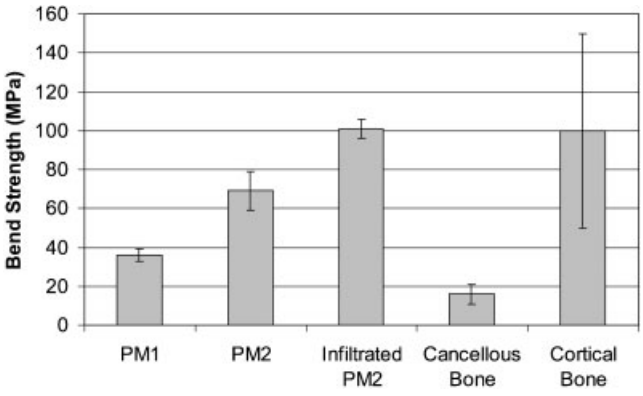

Fig. 10 Three-point bend test results

Figures 11 to 15 show SEM images of PM1 scaffolds at different magnifications and at different time periods (cf. Fig. 7). The images show that the A–W material was covered by a layer of fine needle-like crystals after a period of one day, and that this layer

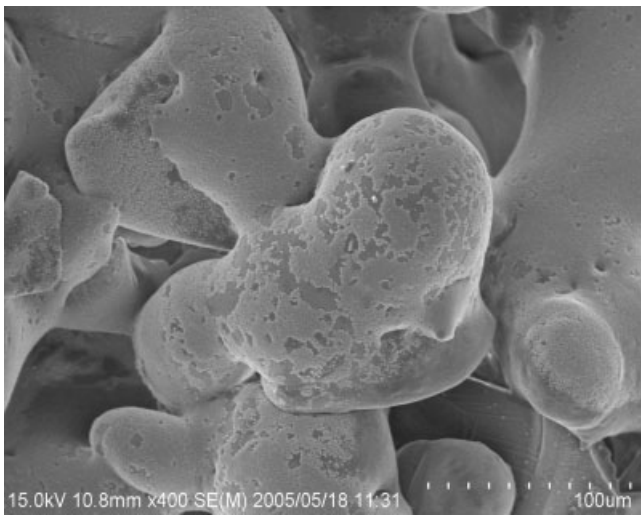

Fig. 11 PM1 scaffold soaked in SBF for 1 day

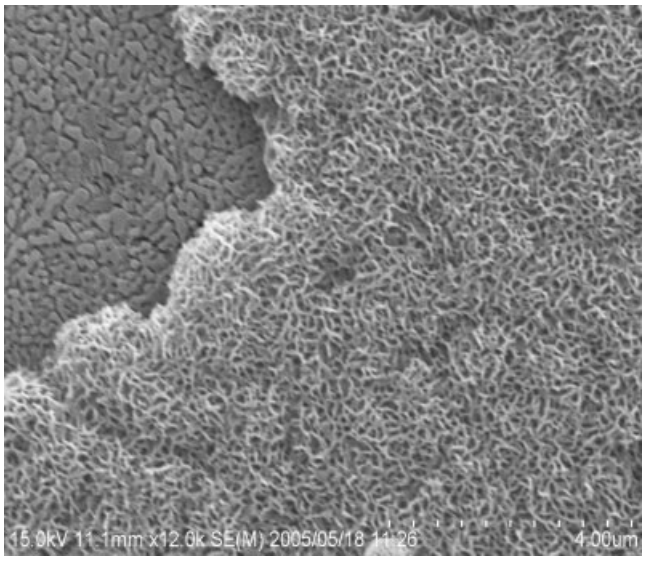

Fig. 12 PM1 scaffold soaked in SBF for 1 day

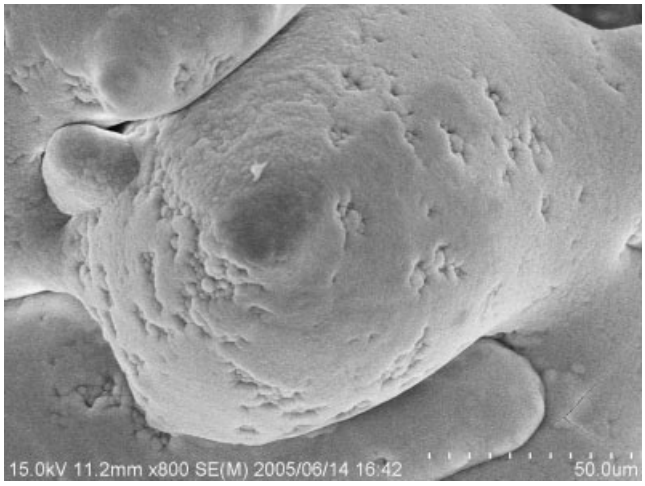

Fig. 13 PM1 scaffold soaked in SBF for 7 days

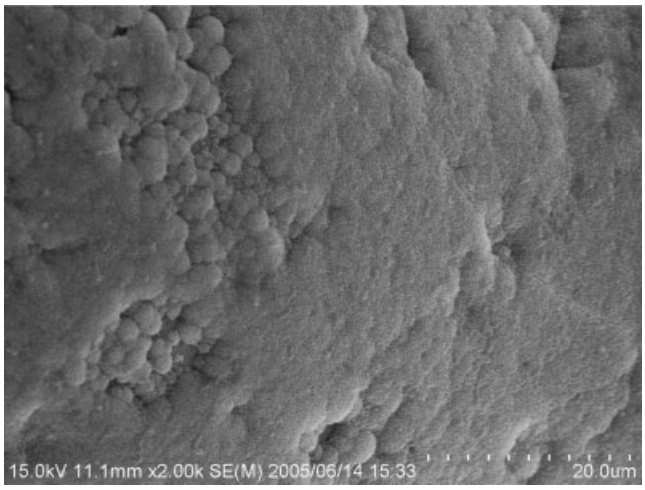

Fig. 14 PM1 scaffold soaked in SBF for 14 days

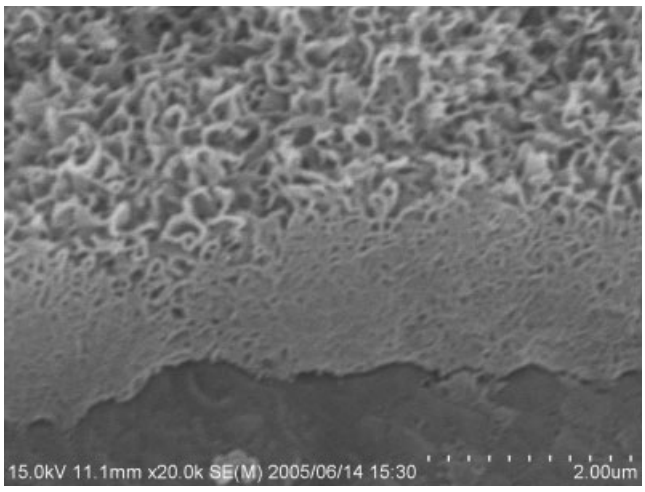

Fig. 15 PM1 scaffold soaked in SBF for 14 days

continued to grow over the 14-day period of soaking. EDX indicated that this layer was rich in Ca and P, indicating the formation of amorphous phosphate and crystalline apatite on the surface of the glasses by consuming the phosphate ions from the SBF fluid (stages 4 and 5 of Hench's mechanism of bioactivity [**9**]). This behaviour is similar to that seen in conventionally processed A–W [**8**] and confirms that processing by indirect SLS has no effect on the *in vitro* behaviour of the material. As an essential condition for glasses and glass–ceramics to bond to living bone is the formation of a bone-like apatite layer on their surface [**2**], the scaffolds exhibit excellent *in vitro* bioactivity.

Figures 16 to 18 show SEM images from SBF tests with infiltrated PM2 scaffolds at different time points and magnifications. It is clear that the behaviour of

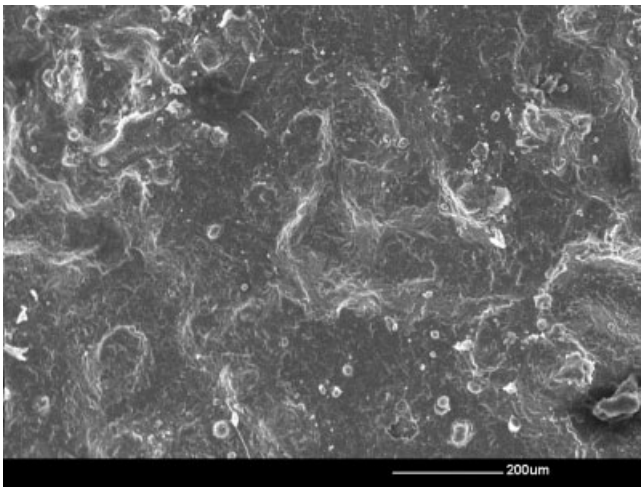

Fig. 16 Infiltrated PM2 scaffold soaked in SBF for 1 day

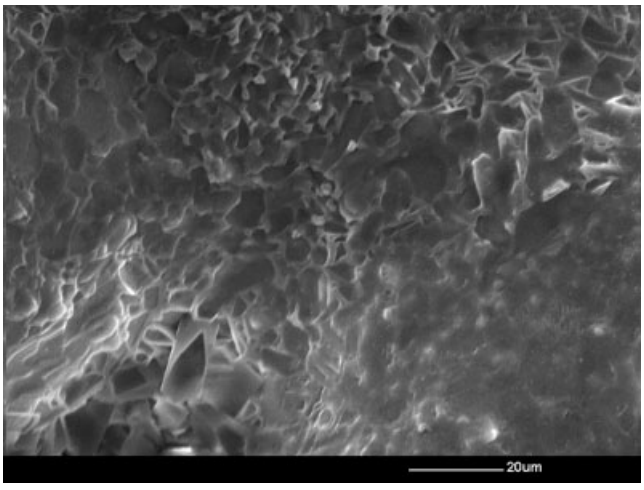

Fig. 17 Infiltrated PM2 scaffold soaked in SBF for 7 days

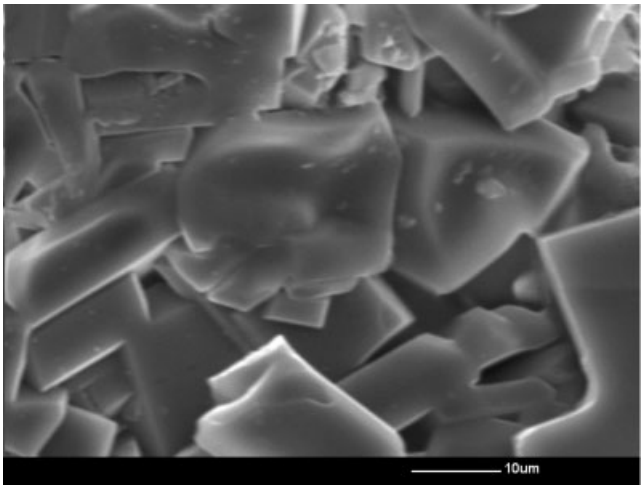

Fig. 18 Infiltrated PM2 scaffold soaked in SBF for 14 days

the infiltrated material is significantly different to that of the uninfiltrated. Plate-like crystals form on the surface, and in addition it was observed that the SBF solution became cloudy after one day of soaking, indicating precipitation. The plate-like structure, although unusual, has been tentatively identified as hydrated calcium orthophosphate, as reported by Clement *et al.* [**10**], with dissolution of the phosphate glass giving rise to the precipitation. While the behaviour shown by the infiltrated material is more complex, it is considered that the behaviour is also indicative of a high level of bioactivity in the material [**11**].

5 DISCUSSION AND CONCLUSIONS

The main aim of the work reported here was to create a hard tissue scaffold using a processing route that would allow for the manufacture of scaffolds which could be personalised to the implant site, which had mechanical properties close to those of natural bone, and which had excellent biological properties. The indirect SLS processing route adopted allows the correct material phases to be evolved in the post-processing step, and the SBF studies have shown that this results in a scaffold with high levels of bioactivity. The processing route also allows for different levels of porosity to be built into the scaffold either as a result of choice of processing route (as has been demonstrated in this paper) or through the manufacture of macro-porous structures (possible through any layer manufacturing route). This means that levels of porosity and mechanical properties can potentially be tailored to a large degree to the implant site. Overall, A–W scaffolds fabricated by indirect SLS are considered to offer excellent potential as hard tissue scaffolds.

REFERENCES

1 **Salgado, A. J., Coutinho, O. P.,** and **Reis, R. L.** Bone tissue engineering state of the art and future trends. *Macromolecular Biosci.*, 2004, **4**, 743–765.

2 **Kokubo, T., Shigematsu, M., Nagashima, Y., Tashiro, M., Nakamura, T.,** and **Yamamuro, T.** Apatite- and wollastonite-containing glass–ceramics for prosthetic application. *Bull. Inst. Chem. Res.*, 1982, **60**, 260–268.

3 **Goodridge, R. D., Dalgarno, K. W.,** and **Wood, D. J.** Indirect selective laser sintering of an apatite–mullite glass–ceramic for potential use in bone replacement applications. *Proc. IMechE, Part H: J. Engineering in Medicine*, 2006, **220**, 57–68.

4 **Kokubo, T.** Bioactive glass ceramics: properties and applications. *Biomaterials*, 1991, **12**, 155–163.

5 **Ohsawa, K., Neo, M., Okamoto, T., Tamura, J.,** and **Nakamura, T.** In vivo absorption of porous apatite- and wollastonite-containing glass–ceramic. *J. Mater. Sci. Mater. Med.*, 2004, **15**, 859–864.

6 **Likitvanichkul, S.** and **Lacourse, W. C.** Apatite–wollastonite glass-ceramics. Part I: crystallization kinetics by differential thermal analysis. *J. Mater. Sci.*, 1998, **33**, 5901–5904.

7 **Lorrison, J. C., Dalgarno, K. W.,** and **Wood, D. J.** Processing of an apatite–mullite glass–ceramic and an hydroxyapatite/phosphate glass composite by selective laser sintering. *J. Mater. Sci. Mater. Med.*, 2005, **16**, 775–781.

8 **Kokubo, T., Kushitani, H., Ohtsuki, C., Sakka, S.,** and **Yamamuro, T.** Chemical reaction of bioactive glass and glass-ceramics with a simulated body fluid. *J. Mater. Sci. Mater. Med.*, 1992, **3**, 79–83.

9 **Jones, J. R.** and **Hench, L. L.** Biomedical materials for new millennium: perspective on the future. *Mater. Sci. Technol.*, 2001, **17**, 891–900.

10 **Clement, J., Planell, J. A., Avila, G.,** and **Martinez, S.** Analysis of the structural changes of a phosphate glass during its dissolution in simulated body fluid. *J. Mater. Sci. Mater. Med.*, 1999, **10**, 729–732.

11 **Xiao, K.** *Indirect selective laser sintering of apatite–wollastonite glass–ceramics.* PhD Thesis, University of Leeds, Leeds, UK, 2007.